Chapter 21

HYBRID COMPUTER SIMULATION OF SEDIMENT TRANSPORT WITH STOCHASTIC TRANSFER AT THE STREAM BED

By

Kousoum S. Sakhan, Graduate Research Assistant, Civil Engineering, Utah Water Research Laboratory, Utah State University, Logan, Utah

J. Paul Riley, Professor, Civil Engineering, Utah Water Research Laboratory, Utah State University, Logan, Utah

and

Kenneth G. Renard, Director, Southwest Watershed Research Center, Agricultural Research Service, U.S. Department of Agriculture, Tucson, Arizona

SYNOPSIS 21-1
CHANNEL DYNAMICS MODEL 21-2
FLUID MASS AND SOLID MASS TRANSPORT EQUATIONS. 21-2
Stochastic Sediment Transfer at the Stream Bed. 21-6
COMPUTATIONAL APPROXIMATIONS 21-19
HYBRID COMPUTER SIMULATION 21-23
Simulation of a Stream Reach. 21-23
Sensitivity Analysis. 21-25
CONCLUDING REMARKS 21-26
PARTIAL LIST OF SYMBOLS. 21-28
REFERENCES 21-31

HYBRID COMPUTER SIMULATION OF SEDIMENT TRAN

WITH STOCHASTIC TRANSFER AT TH TREAM BED[1/]

by

Kousoum S. Sakhan, J. Paul Riley, and Kenneth G. Renard[2/]

SYNOPSIS

In ephemeral streams, the occurrence of translatory waves causes the hydrograph to rise more rapidly, which, in turn, results in channel instability. A simulation model is developed to describe the dynamics of the channel in terms of: (1) two one-dimensional streamflow equations, (2) a one-dimensional sediment transport equations, an equation for the stream bed, and (3) a stochastic sediment transfer at the stream bed which also includes the bed load.

The model as a whole is simulated on a hybrid computer. To demonstrate the operation of the model, real-time simulation is done using hypothetical data for a stream reach 24,000 feet long. The results of this study are presented in graphical form.

1/ The work described herein was funded primarily by the Agricultural Research Service, U.S. Department of Agriculture. The paper was prepared for presentation at a Sediment Symposium to honor Professor Hans Albert Einstein in Berkeley, California, June 17-19, 1971.

2/ Graduate Research Assistant, Civil Engineering, Utah Water Research Laboratory, Utah State University, Logan Utah; Professor, Civil Engineering, Utah Water Research Laboratory, Utah State University, Logan Utah; Director, Southwest Watershed Research Center, Agricultural Research Service, United States Department of Agriculture, Tucson, Arizona.

CHANNEL DYNAMICS MODEL

Existing information is inadequate on channel stability influences. Under present conditions, many stream channels in the Southwestern United States are unstable. The major cause is believed to be the high-intensity, short-duration convective thunderstorms, particularly during the summer season, which result in flash floods moving over coarse-textured alluvial stream beds with very high-intake rates. It has been observed by Renard and Hickock[1/] that the occurrence of translatory waves occur frequently. This phenomenon has a critical influence on the time of rise of the hydrograph, which in turn, affects the stability of the stream channel. The conventional theory of flood routing is inapplicable to these ephemeral streams. Therefore, it is necessary to account for the movement of these waves in order for the model to be descriptive of emphemeral streams. Besides these translatory waves, sediments carried by the flow both as bed load and suspended load make the situation even more complicated.

The present model does not account directly for the movement of the translatory waves that might occur, but, it only gives an approximation to it. An integrated system of sediment flow is viewed as the only solution to the problem of instability of ephemeral stream channels. An effort is made to apply stochastic processes to describe that portion of the process--that is, the movement of sediments at the stream bed--which cannot be adequately described in a deterministic way.

In systems analysis, relationships are customarily displayed graphically. Because of the complexity of the results obtained from the simulations, the graphical results produced by the model permit an insight into the movements of sediments in relation to the flow.

FLUID MASS AND SOLID MASS TRANSPORT EQUATIONS

The three-dimensional equations of conservation of fluid mass, flow momentum, and solid mass in the turbulent flow are

$$\nabla \cdot \vec{V} = 0 \tag{1}$$

$$\rho \frac{d\vec{V}}{dt} = \rho \vec{g} - \nabla p + \mu \nabla^2 \vec{V} + [\nabla \cdot T^{(e)}] \tag{2}$$

$$\frac{\partial c}{\partial t} + \nabla \cdot (c\vec{V}) = \nabla \cdot (e\nabla c) \tag{3}$$

subject to the following boundary conditions (Figure 1)

$$\frac{dF}{dt} = \frac{\partial F}{\partial t} + \vec{V} \cdot \nabla F = \vec{R} \cdot \nabla F \tag{4}$$

$$c \frac{\partial F}{\partial t} - e \nabla c \cdot \nabla F = \vec{N} \cdot \nabla F \tag{5}$$

where $T^{(e)}$ is the Reynolds stress tensor and $F(x, y, z, t) = 0$ is the equation of the moving boundary surface. After space averaging (Sakhan[2]) Equations (1), (2), and (3) reduce to the following one-dimensional equations which describe the conservation of fluid mass, flow momentum, and solid mass in the flow of natural streams with movable boundaries,

$$\frac{\partial A}{\partial t} + \frac{\partial Q}{\partial x} - L - S = 0 \tag{6}$$

$$\frac{\partial Q}{\partial t} + \frac{\partial}{\partial x}\left(\beta \frac{Q^2}{A}\right) + g \frac{\partial}{\partial x}(h_c A) + g A \frac{\partial \eta_1}{\partial x} - \frac{Q}{A}(\beta_L L + \beta_s S)$$
$$+ \frac{1}{\rho} \int_{\sigma_2}^{\sigma_1} \left(\mu \frac{\partial u}{\partial y} - \rho \overline{u'v'}\right) /_{y=\eta_1} dz = 0 \tag{7}$$

$$\frac{\partial}{\partial t}(CA) + \frac{\partial}{\partial x}(CQ) = \frac{\partial}{\partial x}\left(G_{cx} A \frac{\partial C}{\partial x}\right)$$
$$+ \tilde{c}/_{y=\eta_1} \left[S + T \frac{\partial \overset{\sim}{\eta_1}}{\partial t}\right] + N/_{y=\eta_1} \tag{8}$$

in which the terms L, S, and N, as described in the terminology, have negative values if the processes they represent are influent, and positive values if the processes are effluent. The stream coordinates σ_1, σ_2, and η_1 are as shown in Figures 1.a and 1.b. The wavy bar indicates averages over the top width T of flow.

Assuming the bed shear stress in an unsteady flow can be approximated by that in a uniform flow, the last term of Equation (7) can be represented by

$$\frac{1}{\rho} \int_{\sigma_2}^{\sigma_1} \left(\mu \frac{\partial u}{\partial y} - \rho \overline{u'v'}\right) /_{y=\eta_1} dz = \frac{\tau_0 P_w}{\rho} \tag{9}$$

where P_w is the wetted perimeter and τ_o is the mean bed shear stress. For a uniform flow,

$$\tau_o = \gamma R_h S_f \tag{10}$$

where the friction slope S_f can be approximated by the Darcy-Weisbach equation

$$S_f = \frac{Q^2 f}{8g R_h A^2} \tag{11}$$

in which R_h is the hydraulic radius.

The friction factor f in Equation (11) is known to change with the flow and channel characteristics. This friction factor can be decomposed into f' which represents the sand grain roughness and f'' which represents the bed form roughness. For the evaluation of these two friction factors the following two relationships will be adopted:

$$\frac{1}{\sqrt{f'}} = 2 \log_{10} (R_h/D_{50}) + 1.5 \tag{12}$$

and

$$\log_{10} f'' = - .45 - .04 \frac{U}{\sqrt{gD_{50}}} + (.04 \frac{U}{\sqrt{gD_{50}}} - 3.05)$$

$$\exp (- 8 [\log_{10} (R_h/D_{50}) - (1.9 + .04 \frac{U}{\sqrt{gD_{50}}}]) \tag{13}$$

in which D_{50} is the median diameter of the sediment particles at the stream bed. Equation (13) is based on data from several laboratory flume experiments and natural streams which are in regime. For non-regime flows such as the ephemeral stream in the Southwest, it might not be applicable. From field observations, flat beds are of general occurrence. This is due to the wide distribution of the sediment sizes. The bed particles range from rocks down to fine-grained sands. The channels generally have steep slopes. Ripples, dunes, or anti-dunes are not likely to form on steep slopes with highly heterogeneous bed particles.

By following Chen[3]/ and assuming logarithmic velocity distribution in both vertical and lateral directions, the longitudinal sediment dispersivity, G_{cx} in Equation (8), can be derived and expressed as:

$$G_{cx} = \frac{\lambda\kappa}{24} \frac{\sqrt{gS_f}}{R_h} \frac{[\log_e (\frac{h}{\eta_0 - \eta_1}) - 1]^2}{[\log_e (\frac{T/2}{\sigma_0 - \sigma_1})]^2} T^2 \tag{14}$$

in which λ is the ratio of the eddy mass diffusivity to the eddy kinematic viscosity of water, κ is the von Karman universal constant, h is the depth of flow, T is the top width of flow, and η_0 and σ_0 are the distances from the stream bed and the side walls, respectively, where the velocity is zero.

Seepage from initially dry channels following the onset of inundation must be treated as unsaturated flow. However, in a number of situations such as the ephemeral streams in the Southwest where the water depth is relatively large for most of the channel perimeter, the bed material is coarse, and the water table is very deep, piston-like flow with a sharp wetting front and constant hydraulic conductively in the wetted zone would occur. In this type of flow, gravity plays an important role.

If it is assumed that the bottom of the wetted zone is horizontal, the stream lines of seepage are all perpendicular to this bottom, and the wetted zone itself is of constant hydraulic conductivity, then the total seepage can be approximated by a steady state case with different water depths in the channel. The mathematical representation of this seepage will be derived in a complex plane $\Omega = z + i(-y)$ as shown in Figure 2.

Use will be made of the Zhukovsky's function which is expressed as

$$Z = i\Omega + \frac{\omega}{K} = R \exp\left(\frac{\omega}{\alpha}\right) \tag{15}$$

in which $i = \sqrt{-1}$; ω is the complex potential $\omega = \phi + i\psi$, ϕ being the potential function and ψ the stream function; K is the hydraulic conductivity of the stream bed; α is a parameter; and R is a real constant. Considering only one quadrant (quadrant (I) as shown in Figure 2), the function Z can be separated into real and imaginary parts,

$$+ (-y) + \frac{\phi}{K} = R \exp\left(\frac{\phi}{\alpha}\right) \cos\left(\frac{\psi}{\alpha}\right) \tag{16.a}$$

and

$$z + \frac{\psi}{K} = R \exp\left(\frac{\phi}{\alpha}\right) \sin\left(\frac{\psi}{\alpha}\right) \tag{16.b}$$

The following boundary conditions must be satisfied:

1. Along the -y-axis, $\psi = 0$

2. Along the stream bed, $\phi = 0$
3. At the free surface, $+ (-y) + \frac{\phi}{K} = 0$ and $\psi = + \frac{S}{2}$

It can be deduced from Condition 3 that

$$S = \alpha \pi \tag{17}$$

Equating Condition 3 with Equation (16.b) yields

$$z + \frac{S}{2K} = R \exp (+ Ky\pi/S) \tag{18}$$

or

$$z (-y = 0) = \frac{T}{2} = R - \frac{S}{2K} \tag{19}$$

or

$$z (-y = \infty) = - \frac{S}{2K} \tag{20}$$

At the stream bed where $\phi = 0$, Equations (16.a and b) become

$$+ (-y) = R \cos \left(\frac{\psi}{\alpha}\right) \tag{21.a}$$

and

$$z + \frac{\psi}{K} = R \sin \left(\frac{\psi}{\alpha}\right) \tag{21.b}$$

At the stream bed where $\psi = 0$, $\phi = 0$, the real constant can be evaluated as

$$R = + (-y) = - h_{max} (t) \tag{22}$$

Equating Equations (19) and (22) yields the volumetric rate of seepage per unit length of channel

$$S = - K (T + 2 h_{max}) \tag{23}$$

Because of the random nature of the driving mechanism, which is the flow turbulence, the rate of transfer of sediment N should be described by a stochastic process. This process is treated in the following section.

Stochastic Sediment Transfer at the Stream Bed

To formulate an integrated sediment movement model, the suspended sediment model must be connected to the bed scouring mod-

el by some expressions describing the sediment transfer in the stream bed region.

The term $\tilde{c}/_{y=\eta_1}\ T\ \frac{\partial \eta_1}{\partial t} + N/_{y=\eta_1}$ in Equation (8) plays the role of source or sink to the suspended sediment. Through this term the suspended sediment model can be connected to the bed scouring model. The bed scouring model is formulated by integrating the boundary condition (5) with respect to z from $z=\sigma_2$ to $z=\sigma_1$ as

$$\int_{\sigma_2}^{\sigma_1} c/_{y=\eta_1} \frac{\partial \eta_1}{\partial t}\, dz + \int_{\sigma_2}^{\sigma_1} \left(-e_x \frac{\partial c}{\partial x}\frac{\partial \eta_1}{\partial x} + e_y \frac{\partial c}{\partial y} - e_z \frac{\partial c}{\partial z}\frac{\partial \eta_1}{\partial z}\right) dz = \int_{\sigma_2}^{\sigma_1} \left(N_x \frac{\partial \eta_1}{\partial x} - N_y + N_z \frac{\partial \eta_1}{\partial z}\right) dz \tag{24}$$

or

$$\tilde{c}/_{y=\eta_1}\ T\ \frac{\partial \tilde{\eta}_1}{\partial t} + \frac{\partial}{\partial x}\left(Q_{B\ vol}\right) + N = 0 \tag{25}$$

in which the volumetric bed load discharge, $Q_{B\ vol}$, is defined as:

$$\frac{\partial}{\partial x}\left(Q_{B\ vol}\right) = \int_{\sigma_2}^{\sigma_1} \left(-e_x \frac{\partial c}{\partial x}\frac{\partial \eta_1}{\partial x} + e_y \frac{\partial c}{\partial y} - e_z \frac{\partial c}{\partial z}\frac{\partial \eta_1}{\partial z}\right) dz \tag{26}$$

and the volumetric rate of sediment exchange between the stream bed and the suspended load, Q_{BS}, is defined as:

$$N/_{y=\eta_1} = \frac{\partial}{\partial x}\left(Q_{BS}\right) = \int_{\sigma_2}^{\sigma_1} \left(N_x \frac{\partial \eta_1}{\partial x} - N_y + N_z \frac{\partial \eta_1}{\partial z}\right) dz \tag{27}$$

Since it is impossible to obtain an analytical evaluation of the right-hand side of Equation (26) and the term N, a stochastic approach is proposed.

At the interface between the flow region and the stream bed, there are three distinct states: (A) the suspended state, (B) the bed load state, and (C) the immobile bed state (Figure 3), at time T, a sediment particle may be in any one of these three states.

The probability that a particle will move from one state to another or remain in a particular state is termed its transition probability. The future transition probabilities of a sediment particle are independent of its transition probabilities in the past (a property of the Markov Processes). For example, if a particle is in state (A) at time θ and in state (B) at time ϕ, the probability that it is in state (C) at time t is given by the appropriate transition probabilities as follows:

$$P_{AC}(\theta,t) = P_{AB}(\theta,\phi)\, P_{BC}(\phi,t) \tag{28}$$

Generally, since the events corresponding to Equation (28) for different middle states are mutually exclusive, the probability of going from state (A) at time θ to state (C) at time t is

$$P_{AC}(\theta,t) = \sum_{i=A}^{C} P_{Ai}(\theta,\phi)\, P_{iC}(\phi,t) \tag{29}$$

Equation (29) is known as the Chapman-Kolmogorov equation for a non-homogeneous Markov process. If it is defined that

$$\psi_{AB}\,\Delta t + 0(\Delta t) = P_r\,[\text{a particle in state (A) at time } \phi \text{ will be in state (B) at time } \phi + \Delta t] \tag{30.a}$$

$$\psi_{AC}\,\Delta t + 0(\Delta t) = P_r\,[\text{a particle in state (A) at time } \phi \text{ will be in state (C) at time } \phi + \Delta t] \tag{30.b}$$

and

$$1 + \psi_{AA}\,\Delta t + 0(\Delta t) = P_r\,[\text{a particle in state (A) at time } \phi \text{ will remain in state (A) during the interval } (\phi, \phi + \Delta t)] \tag{30.c}$$

then it is clear that

$$\psi_{AA} = -\sum_{i=B}^{C} \psi_{Ai} \leq 0 \tag{31}$$

If ψ_{AA} is zero, then state Ⓐ is absorbing, that is, the sediment particle is always in suspension. This case is not expected to happen in a natural stream.

Now consider two contiguous time intervals, (θ,t) and $(t, t + \Delta t)$. Using the definitions in Equations (30.a-c) with Equation (29) yields

$$P_{AA}(\theta, t + \Delta t) = P_{AA}(\theta,t)(1 + \psi_{AA}\Delta t) + P_{AB}(\theta,t)\psi_{BA}\ t + P_{AC}(\theta,t)\psi_{CA}\Delta t + 0(\Delta t) \quad (32.a)$$

$$P_{AB}(\theta, t + \Delta t) = P_{AA}(\theta,t)\psi_{AB}\Delta t + P_{AB}(\theta,t)(1 + \psi_{BB}\Delta t) + P_{AC}(\theta,t)\psi_{CA}\Delta t + 0(\Delta t) \quad (32.b)$$

and

$$P_{AC}(\theta, t + \Delta t) = P_{AA}(\theta,t)\psi_{AC}\Delta t + P_{AB}(\theta,t)\psi_{BC}\Delta t + P_{AC}(\theta,t)(1 + \psi_{CC}\Delta t) + 0(\Delta t) \quad (32.c)$$

Dividing Equations (32.a-c) by Δt and taking the limit as Δt approaches zero results in the following relationships:

$$\frac{\partial}{\partial t} P_{AA}(\theta,t) = P_{AA}(\theta,t)\psi_{AA}(t) + P_{AB}(\theta,t)\psi_{BA}(t) + P_{AC}(\theta,t)\psi_{CA}(t) \quad (33.a)$$

$$\frac{\partial}{\partial t} P_{AB}(\theta,t) = P_{AA}(\theta,t)\psi_{AB}(t) + P_{AB}(\theta,t)\psi_{BB}(t) + P_{AC}(\theta,t)\psi_{CA}(t) \quad (33.b)$$

$$\frac{\partial}{\partial t} P_{AC}(\theta,t) = P_{AA}(\theta,t)\psi_{AC}(t) + P_{AB}(\theta,t)\psi_{BC}(t) + P_{AC}(\theta,t)\psi_{CC}(t) \quad (33.c)$$

Equations (33.a-c) are known as the forward Kolmogorov differential equations. They are subject to the following initial conditions

$$P_{Ai}(0,0) = \delta_{Ai}, \quad i = A, B, C \tag{34}$$

where δ_{Ai} is the Kronecker delta symbol.

The ψ's are the intensities of sediment transfer which are the main keys to the concept of stochastic sediment transfer at the interface. They are functions of the instantaneous local hydrodynamic properties. Considering that the time interval $(0,t)$ is very short, then it can be assumed that the ψ's are constant over this interval. However, in general, the ψ's are time-dependent.

The Kolmogorov differential equations for P_{BA}, P_{BB}, P_{BC}, P_{CA}, P_{CB}, and P_{CC} may be derived in a similar manner and presented in matrix format. Let the transition probability matrix be

$$\vec{P}(0,t) = \begin{array}{c} \\ A \\ B \\ C \end{array} \begin{array}{c} \begin{array}{ccc} A & B & C \end{array} \\ \begin{bmatrix} P_{AA}(0,t) & P_{AB}(0,t) & P_{AC}(0,t) \\ P_{BA}(0,t) & P_{BB}(0,t) & P_{BC}(0,t) \\ P_{CA}(0,t) & P_{CB}(0,t) & P_{CC}(0,t) \end{bmatrix} \end{array} \tag{35}$$

and let the sediment transfer intensity matrix be

$$\vec{\psi}(t) = \begin{array}{c} \\ A \\ B \\ C \end{array} \begin{array}{c} \begin{array}{ccc} A & B & C \end{array} \\ \begin{bmatrix} \psi_{AA}(t) & \psi_{AB}(t) & \psi_{AC}(t) \\ \psi_{BA}(t) & \psi_{BB}(t) & \psi_{BC}(t) \\ \psi_{CA}(t) & \psi_{CB}(t) & \psi_{CC}(t) \end{bmatrix} \end{array} \tag{36}$$

Then the Chapman-Kolmogorov equation becomes

$$\vec{P}(0,t) = \vec{P}(0,\phi)\,\vec{P}(\phi,t) \tag{37}$$

In a similar manner the forward Kolmogorov differential equations become

$$\frac{\partial}{\partial t} \vec{P}(\theta, t) = \vec{P}(\theta, t)\, \vec{\psi}(t) \tag{38}$$

subject to the initial conditions

$$\vec{P}(\theta, t) = \vec{I} \tag{39}$$

where $\vec{I}$ is the identity matrix.

The task now is to determine the intensity matrix $\vec{\psi}(t)$. Referring to Figure (3) there are six from state-to-state transfers and three within-state transfers. The terms state and zone should not be confused. With the complexity regarding the arrangement of sediment particles at the stream bed and the instantaneous local hydrodynamic forces, it is impossible to draw a physical boundary between the bed load zone and the suspended load zone. However, it is possible to avoid this problem by considering states of a sediment particle which do not have physical boundaries, but rather "process boundaries." The process boundaries are defined by the following relations (40 through 45) which define the process conditions for transfer between states. For example, relationships (40 and 45) define the process boundaries for state (B).

(AB) - Transfer from suspended load state to bed load state occurs when the local upward hydrodynamic force $F_y(v'_{up})$ is less than the vertical resisting force $F(m)$ due to sediment mass,

$$F_y(v'_{up}) \leq F_y(m) \tag{40}$$

(AC) - Transfer from suspended load state directly to immobile bed state occurs when

$$F_y(v'_{up}) \leq F_y(m) \tag{41}$$

(BA) - Transfer from bed load state to suspended load state takes place when

$$F_y(v'_{up}) > F_y(m) \tag{42}$$

(BC) - Transfer from bed load state to immobile bed state occurs when

$$F_x(\tau_o, u') \leq F_x(m, \tau_o) \tag{43}$$

(CA) - Transfer from immobile bed state directly to suspended load occurs when

$$F_y(v'_{up}) > F_y(m) \tag{44}$$

(CB) - Transfer from immobile bed state to bed load state occur when

$$F_x(\tau_o, u') > F_x(m, \tau_o) \tag{45}$$

As can be seen from Equation (31), within-state transfers are functions of transfer between states.

Let u_{for} be the forward velocity in the horizontal direction, v_{rise} the rise velocity, and v_{fall} the fall velocity of the particle at the interface region. If a sediment particle moved with one of these three velocities, how many fictitious sediment particles similar to that real particle would move at maximum intensity, past a single "serving counter" per unit time? Let D be the diameter of the particle. Then there should be, for example, u_{for}/D particles per unit time which move in the forward horizontal direction. It is difficult to visualize why fictitious particles are being considered. Since the probability of changing states or staying within a particular state corresponds to a single particle, the best illustration of this process is to visualize a queue of particles identical to that single particle being "served by a single counter." Under this reasoning, the intensity function matrix (36) becomes

$$\vec{\psi}(t) = \begin{array}{c} \\ A \\ B \\ C \end{array} \begin{array}{c} \begin{array}{ccc} A & B & C \end{array} \\ \begin{bmatrix} -\left(\frac{v_{fall}}{D} + \frac{v_{fall}}{D}\right) & \frac{v_{fall}}{D} & \frac{v_{fall}}{D} \\ \frac{v_{rise}}{D} & -\left(\frac{v_{rise}}{D} + \frac{v_{fall}}{D}\right) & \frac{v_{fall}}{D} \\ \frac{v_{rise}}{D} & \frac{u_{for}}{D} & -\left(\frac{v_{rise}}{D} + \frac{u_{for}}{D}\right) \end{bmatrix} \end{array} \tag{46}$$

subject to the process conditions (40 through 45). The entry that does not meet its respective process condition vanishes.

To evaluate the above matrix, the three sediment particle velocities, u_{for}, v_{rise}, and v_{fall}, must be determined. In natural streams, various bed configurations are formed, depending upon the flow conditions, the characteristics of the bed material, and the stream geometry. In turn, bed features affect "wall" turbulence near the bed, which is a primary entrainment mechanism for sediment particles. Another important entrainment mechanism is the mean bed shear stress. In the interface region of natural streams, the Newtonian law of motion is valid. Thus,

$$\vec{F} = \frac{d}{dt}(m\,\vec{V}_p) \tag{47}$$

in which $\vec{F}$ is the total force vector on the particle; m is the mass of the particle, which is constant; and $\vec{V}_p$ is the velocity vector of the particle. Integrating Equation (47) from time t_1 to time t_2 yields

$$\int_{t_1}^{t_2} \vec{F}\,dt = m\,\vec{V}_{p_2} - m\,\vec{V}_{p_1}$$

where $\int_{t_1}^{t_2} \vec{F}\,dt$ is known as the impulse of the force $\vec{F}$ on the particle. Decomposing the force $\vec{F}$ into two parts, the hydrodynamic force, $\vec{F}_{hydro}$, and the resisting force, $\vec{F}_{resist}$, and integrating Equation (48) over the entire surface, Λ, of the bed feature yields

$$\int_{\Lambda}\int_{t_1}^{t_2} \vec{F}_{hydro}\,dt\,d + \int_{\Lambda}\int_{t_1}^{t_2} \vec{F}_{resist}\,dt\,d\Lambda = m\int_{\Lambda} (\vec{V}_{p_2} - \vec{V}_{p_1})\,d\Lambda \tag{49}$$

Let $\dot{\widetilde{F}}_{hydro}$, $\vec{\widetilde{F}}_{resist}$, $\widetilde{(\vec{V}_{p_2} - \vec{V}_{p_1})}$, and $\tilde{\Lambda}$ be the averages of $\vec{F}_{hydro}$, $\vec{F}_{resist}$, $(\vec{V}_{p_2} - \vec{V}_{p_1})$, and Λ in the domain Λ and t, respectively. Then Equation (49) becomes

$$\tilde{\Lambda}\,(t_2 - t_1)\,(\vec{\widetilde{F}}_{hydro} + \vec{\widetilde{F}}_{resist}) = \tilde{\Lambda} m\,\widetilde{(\vec{V}_{p_2} - \vec{V}_{p_1})} \tag{50}$$

In natural streams, the longitudinal and the vertical components of the particle motion are usually the predominant processes. Hence, from Equation (50),

$$u_p = (\widetilde{u_{p_2} - u_{p_1}}) = \frac{t_2 - t_1}{m} (\widetilde{F}_{hydro\ x} + \widetilde{F}_{resist\ x}) \qquad (51)$$

and

$$v_p = (\widetilde{v_{p_2} - v_{p_1}}) = \frac{t_2 - t_1}{m} (\widetilde{F}_{hydro\ y} + \widetilde{F}_{resist\ y}) \qquad (52)$$

where u_p and v_p are the relative longitudinal and vertical particle velocities. The time of action $(t_2 - t_1)$ of the summation of forces $(\widetilde{F}_{hydro} + \widetilde{F}_{resist})$ is assumed to be, as can be deduced from the reasoning to obtain the intensity function matrix (46),

$$t_2 - t_1 = \frac{D}{\pm (\widetilde{\vec{V}_{p2} - \vec{V}_{p1}})} \qquad (53)$$

Because of the time of action $(t_2 - t_1)$ should always be positive, the plus and minus signs in front of the expression $(\widetilde{\vec{V}_{p2} - \vec{V}_{p1}})$ in Equation (53) are necessary.

Substituting Equation (53) into Equations (51) and (52) yields

$$\pm u_p^2 = \frac{D}{m} (\widetilde{F}_{hydro\ x} + \widetilde{F}_{resist\ x}) \qquad (54)$$

and

$$\pm v_p^2 = \frac{D}{m} (\widetilde{F}_{hydro\ y} + \widetilde{F}_{resist\ y}) \qquad (55)$$

Since sediment particles are sheared over a gravity bed in order to move in the longitudinal direction, one would expect that the particle-to-particle interaction is far greater in the longitudinal direction than in the vertical direction. Then the longitudinal resisting force for a spherical particle can be expressed as

$$\widetilde{F}_{resist\ x} = -(\gamma_s - \gamma) \frac{\pi}{6} D^3 \tan \alpha \qquad (56)$$

in which $\tan \alpha$ is the dynamic friction factor, which as a result of Bagnold's experiments4/ can be expressed as

$$\tan \alpha = .375 + .375 \exp \left[-.00084 \left(\frac{\gamma_s D^2 \tau_0}{14 g \mu^2}\right) - 100)\right] \qquad (57)$$

where μ is the fluid dynamic viscosity.

Since the particle-to-particle interaction is negligible in the vertical direction, the vertical resisting force is due only to the submerged weight of the particle, or

$$F_{resist\ y} = -(\gamma_s - \gamma)\frac{\pi}{6}D^3 \tag{58}$$

The total hydrodynamic force is the mean bed shear stress, $-\rho\,\overline{u'v'}$, superimposed by stresses resulting from turbulent fluctuations u' and v'. Thus,

$$F_{hydro\ x} = \frac{\pi}{4}D^2\,\frac{1}{2}\,C_{Dx}\,\frac{\gamma}{g}\,(\overline{u'^2} - \overline{u'v'}) \tag{59}$$

and

$$F_{hydro\ y} = \frac{\pi}{4}D^2\,\frac{1}{2}\,C_{Dy}\,\frac{\gamma}{g}\,\overline{v'^2_{up}} \tag{60}$$

in which C_{Dx} and C_{Dy} are the drag coefficients in the longitudinal and vertical directions, respectively, and $\overline{v'^2_{up}}$ is the mean-square of the upward velocity fluctuation which is derived and expressed as:

$$\overline{v'^2_{up}} = 2.415\,\overline{v'^2} \tag{61}$$

Now let ϕ_x and ϕ_y be the correlation functions between the root-mean-square velocity fluctuations $\sqrt{\overline{u'^2}}$ and $\sqrt{\overline{v'^2}}$ and the root-mean-square shear velocity $\sqrt{-\overline{u'v'}}$, or

$$\phi_x = \frac{\sqrt{\overline{u'^2}}}{-\overline{u'v'}} \tag{62}$$

and

$$\phi_y = -\frac{\sqrt{\overline{v'^2}}}{\overline{u'v'}} \tag{63}$$

Substituting Equations (53), (54), (56), (57), (61), (62), and (64) into Equations (51) and (52) yields

$$\Delta u_p^2 = \frac{3}{4}\,g\,\frac{C_{Dx}}{\gamma_s}\,(\phi^2_{x/y=\eta_1} + 1)\,\tau_0 - g\,D\,\left(\frac{\gamma_s-\gamma}{\gamma_s}\right)\tan\alpha \tag{64}$$

and

$$Q_{B\ vol}(x, t) = BD_{mean}\,[C_A(x, t-\delta t)\,\psi_{AB}(x, t-\tfrac{1}{2}\delta t)\,P_{AB}(x, t-\tfrac{1}{2}\delta t) + C_C(x, t-\delta t)\,\psi_{CB}(x, t-\tfrac{1}{2}\delta t)\,P_{CB}(x, t-\tfrac{1}{2}\delta t) + C_B(x-x, t-\delta t)\,|\,\psi_{BB}(x-\delta x, t-\tfrac{1}{2}\delta t)\,|\,P_{BB}(x-\delta x, t-\tfrac{1}{2}\delta t) - C_B(x, t-\delta t)\,[\psi_{BA}(x, t-\tfrac{1}{2}\delta t)\,P_{BA}(x, t-\tfrac{1}{2}\delta t) + |\,\psi_{BB}(x, t-\tfrac{1}{2}\delta t)|\,P_{BB}(x, t-\tfrac{1}{2}\delta t) + \psi_{BC}(x, t-\tfrac{1}{2}\delta t)\,P_{BC}(x, t-\tfrac{1}{2}\delta t)]] \quad (72)$$

where B is the effective width of the channel in which the transfer of sediments at the stream bed occurs. For a trapezoidal channel, the effective width should be the bottom width of the channel.

Having arrived at this point, a question still remains. Is the Kolmogorov system (38), which describes Markov processes with time-dependent transition probabilities, a valid system to describe the stochastic sediment transfer at the interface? In other words, is the time spent within each state and from state-to-state exponentially distributed? Exponential distribution is a necessary, though not sufficient, condition of a Markov process and since the time of particle stay or transfer is a function of the instantaneous particle velocity, this velocity has to possess a distribution which belongs to the exponential family.

To see that the instantaneous particle velocity, $\vec{V}_p$, has an exponential distribution, let $F(\vec{V}_p)$ be its distribution function with a range, Γ, or

$$F(\vec{V}_p) = \int_{\Gamma} f(\vec{V}_p)\, d\,\vec{V}_p \quad (73)$$

Going back to Equations (64) and (65) it can be seen that, at the interface,

$$\vec{V}_1' = +\sqrt{K_2\,\vec{V}_p^2 + K_2},\ \vec{V}_2' + -\sqrt{K_1\,\vec{V}_p^2 + K_2} \quad (74)$$

in which K_1 and K_2 are coefficient scalars. Equation (74) indicates that the density function of the random variable $\vec{V}_p$ is a double-valued function. Therefore, the density function $f(\vec{V}_p)$ can be obtained by partial differentiation of Equation (73) as

$$f(\vec{V}_p) = \frac{\partial F(\vec{V}_p)}{\partial \vec{V}_1'} \left| \frac{d\vec{V}_1'}{d\vec{V}_p} \right| + \frac{\partial F(\vec{V}_p)}{\partial \vec{V}_2'} \left| \frac{d\vec{V}_2'}{d\vec{V}_p} \right| \tag{75}$$

At the stream bed, the horizontal fluctuating velocity u' is a Gaussian random process, but the vertical fluctuating velocity v', which is asymmetric as previously described, possesses a probability density distribution curve which is skewed to the side of lower values. These two fluctuations have probability density distributions which belong to the exponential family. Hence, for generalization,

$$\frac{\partial F(\vec{V}_p)}{\partial \vec{V}_1'} = F(\vec{\Omega}_1)\ F(\vec{X}_1) \exp\left[\sum_{i=1}^{2} G_i(\vec{\Omega}_1)\ H_i(\vec{X}_1)\right] \tag{76}$$

and

$$\frac{\partial F(\vec{V}_p)}{\partial \vec{V}_2'} = F(\vec{\Omega}_2)\ F(\vec{X}_2) \exp\left[\sum_{i=1}^{2} G_i(\vec{\Omega}_2)\ H_i(\vec{X}_2)\right] \tag{77}$$

in which $\vec{\Omega}$ is the parameter vector and $\vec{X}$ is the vector containing the random variables u' and v'.

Differentiating Equation (74) with respect to $\vec{V}_p$ yields

$$\left| \frac{d\vec{V}_1'}{d\vec{V}_p} \right| = \left| \frac{d\vec{V}_2'}{d\vec{V}_p} \right| = \frac{K_1 \sqrt{K_3 \vec{V}'^2 + K_4}}{\vec{V}'} \tag{78}$$

in which K_3 and K_4 are coefficient scalars (See Equations (64) and (65).

Then substituting Equations (76), (77), and (78) into Equation (75) yields

$$f(\vec{V}_p) = \frac{K_1 \sqrt{K_3 \vec{V}'^2 + K_4}}{\vec{V}'} \sum_{j=1}^{2} F(\vec{\Omega}_j)\ F(\vec{X}_j) \exp$$

$$\left[\sum_{i=1}^{2} G_i(\vec{\Omega}_j)\ H(\vec{X}_j)\right] \tag{79}$$

Equation (79) indicates the $f(\vec{V}_p)$ has a distribution which belongs to the exponential family, and therefore suggests that it might be described by a Markov process with discrete states in continuous time. If this is the case, the Kolmogorov system (38) is a valid description of stochastic sediment transfer at the stream bed as was assumed in the development of this part of the model.

COMPUTATIONAL APPROXIMATIONS

The essence of the model developed is a system of one-dimensional equations which describe the water flow and the associated sediment movement within a stream channel. The model development is based upon the following sets of equations: (1) those which describe the conservation of fluid mass and flow momentum, (2) those which describe the conservation of sediment mass in the flow, and (3) the Kolmogorov differential equations.

To obtain a high-accuracy approximation in the solution of Equations (6) and (7), the one-step Lax-Wendroff scheme is adopted. Assuming β, β_L, and β_s are all equal to one, Equations (6) and (7) are rewritten in the following form,

$$\frac{\partial \vec{W}}{\partial t} + \frac{\partial F(\vec{W})}{\partial x} + \vec{K} = 0 \tag{80}$$

where

$$\vec{W} = \begin{bmatrix} A \\ Q \end{bmatrix}, \quad F(\vec{W}) = \begin{bmatrix} Q \\ \frac{Q^2}{A} + gh_c A \end{bmatrix},$$

$$\vec{K} = \begin{bmatrix} -S - L \\ gA\frac{\partial n_1}{\partial x} + gAS_f - \frac{Q}{A}(S+L) \end{bmatrix} \tag{81}$$

The vector $\vec{W}$ can be expressed in Taylor series as follows

$$\vec{W}_n^{j+1} = \vec{W}_n^j + \Delta t \left(\frac{\partial \vec{W}}{\partial t}\right)_n^j + \frac{\Delta t^2}{2}\left(\frac{\partial^2 \vec{W}}{\partial t^2}\right)_n^j + \ldots \tag{82}$$

in which the subscript n denotes a space grid point and the superscript j denotes a time grid point in the time-space grid network.

Since this is an explicit scheme in time, t, the second-order term is preserved in order to obtain high order accuracy.

Equation (82) can also be written

$$\begin{aligned} \vec{W}_n^{j+1} = \vec{W}_n^j &- \Delta t \left[\frac{\partial F(\vec{W})}{\partial x} + \vec{K}\right]_n^j \\ &+ \frac{\Delta t^2}{2}\left[\frac{\partial}{\partial x}\left[\left[J_F\left[\frac{\partial F(\vec{W})}{\partial x} + \vec{K}\right]\right]\right]\right]_n^j \\ &+ \frac{\Delta t^2}{2}\left[J_K\left[\frac{\partial F(\vec{W})}{\partial x} + \vec{K}\right]\right]_n^j \end{aligned} \tag{83}$$

in which $\vec{J}_F$ and $\vec{J}_K$ are the Jacobians of $F(\vec{W})$ and $\vec{K}$ with respect to $\vec{W}$, respectively, or

$$\vec{J}_F = \begin{bmatrix} 0 & 1 \\ \frac{\partial}{\partial A}(gh_cA) - (\frac{Q}{A})^2 & 2(\frac{Q}{A}) \end{bmatrix} \tag{84}$$

and

$$\vec{J}_K = \begin{bmatrix} -\frac{\partial S}{\partial A} & 0 \\ g\frac{\partial n}{\partial x} + gS_f + gA\frac{\partial S_f}{\partial A} + \frac{Q}{A^2}(S+L) - \frac{Q}{A}\frac{\partial S}{\partial A} & gA\frac{\partial S_f}{\partial Q} - \frac{S+L}{A} \end{bmatrix} \tag{85}$$

Because the space derivatives are of first order, they are approximated by centered differences. Then Equation (83) can be expanded into a finite-difference form as

$$\begin{aligned} \vec{W}_n^{j+1} = \vec{W}_n^j &- \frac{\Delta t}{2\Delta x}\left[F_{n+1}{}^j(\vec{W}) - F_{n-1}{}^j(\vec{W})\right] - \Delta t\,\vec{K}_n{}^j \\ &+ \frac{\Delta t^2}{2\Delta x^2}\left[\vec{J}_{F\,n+\frac{1}{2}}^{\,j}\left[F_{n+1}{}^j(\vec{W}) - F_n^j(\vec{W})\right]\right. \\ &\left. - \vec{J}_{F\,n-\frac{1}{2}}^{\,j}\left[F_n^j(\vec{W}) - F_{n-1}{}^j(\vec{W})\right]\right] \\ &+ \frac{\Delta t^2}{2\Delta x}\left[\vec{J}_{F\,n+\frac{1}{2}}^{\,j}\,\vec{K}_{n+\frac{1}{2}}^{\,j} - \vec{J}_{F\,n-\frac{1}{2}}^{\,j}\,\vec{K}_{n-\frac{1}{2}}^{\,j}\right] + \frac{\Delta t^2}{2}\vec{J}_{Kn}{}^j\,\vec{K}_n^j \\ &+ \frac{\Delta t^2}{4\Delta x}\vec{J}_{Kn}^{\,j}\left[F_{n+1}{}^j(\vec{W}) - F_{n-1}{}^j(\vec{W})\right] \end{aligned} \tag{86}$$

Using the necessary condition and the third and the fourth sufficient conditions of von Newmann, and the Fourier series method, Sakhan2/ has shown that the following criteria must be met for stability in the solution,

$$\left[(\frac{Q}{A})_{max} + \sqrt{g\frac{\partial}{\partial A}(h_cA)_{max}}\right]\frac{\Delta t}{\Delta x} \le 1 \tag{87}$$

and

$$\Delta t \le \frac{2}{|\vec{J}_K|} \tag{88}$$

The stability criterion for Δt, Equation (88), reflects the effect of the forcing function K, which contains lateral inflow, seepage, channel slope, and bed shear stress, on the stability in the solution. Therefore, an approximation to this function must be made with care if the time step Δt is chosen larger than that specified by the criterion (88). It is probable that the method becomes unstable just because of this forcing function.

There are several possible ways to approximate the solution to Equation (8) which is a variable-coefficient parabolic partial differential equation. Any method would give a good approximation provided it is stable and convergent to the real solution as the time step Δt and the space step Δx used in the difference scheme approach zero. The following difference scheme will be used in this analysis.

$$
\begin{aligned}
C_n^{j+1} A_n^{j+1} = {} & \frac{1}{2}\left(C_{n+1}^j A_{n+1}^j + C_{n-1}^j A_{n-1}^j\right) \\
& - \frac{\Delta t}{2\Delta x}\left[(1+\alpha)\, C_{n+1}^j Q_{n+1}^j - 2\alpha\, C_n^j Q_n^j\right. \\
& \left. - (1-\alpha)\, C_{n-1}^j Q_{n-1}^j\right] + \frac{\Delta t}{2\Delta x^2}\left[\left(G_{cx_{n+1}}^{\ j} A_{n+1}^j\right.\right. \\
& \left. + G_{cx_n}^{\ j} A_n^j\right)\left(C_{n+1}^j - C_n^j\right) \\
& \left. - \left(G_{cx_n}^{\ j} A_n^j + G_{n-1}^j A_{n-1}^j\right)\left(C_n^j - C_{n-1}^j\right)\right] \\
& + \Delta t\, \tilde{C}_{y=n_1}^{\ j}\, S_n^j \\
& - \frac{\Delta t}{2\Delta x}\left(Q_B\, vol_{n+1}^{j+1} - Q_B\, vol_{n-1}^{j+1}\right)
\end{aligned}
\tag{89}
$$

where α (=-1, 0, 1) is the weighting operator. Given initial and boundary values, this equation can be used to obtain the volumetric suspended sediment concentration.

For $\alpha = 0, -1$, the Von Newmann condition is always satisfied. For $\alpha = 1$, the stability criterion for Equation (89) requires that the space step must satisfy

$$
\Delta x \leq \frac{4\, G_{cx}}{U + \sqrt{U^2 + 8\, G_{cx}/\Delta t}} \tag{90}
$$

The Kolmogorov differential equations (38) form a system of three sets, each having three equations because the nine variable coefficients, which represent the intensities of sediment motion at the stream bed, $\psi(t)$, are the same for every set. This system is particularly suited for a direct solution on an analog computer because the intensities of sediment motion within each state, $\psi(t)_{ii}$, are negative (Equation 31). This causes the errors associated with the computation to decay exponentially with time, as it will be analyzed in the next section. The analog circuit diagram for this system is shown in Figure 4. It should be noted that the nine variable coefficients which represent the intensities of sediment motion at the stream bed, $\psi(t)$, are the same for every set. Therefore, the same analog circuitry as shown in Figure 4 may be used to integrate the other two sets of equations to obtain the remaining six probabilities. Only the initial conditions, which are input into the analog integrators to correspond with the probabilities being computed, need to be changed.

The outputs from the three integrators, as shown in Figure 4 represent a set of three computed probabilities. After the integration is carried on for a finite period of time, which is equivalent to the product of the time step Δt and the integration time scale factor, the three probabilities are sampled and stored in the digital computer memory, after sampling the integration is stopped. Then after resetting proper initial conditions, the integration for the other three probabilities will be carried out, and the process will be repeated as many times as it is desired. The integration time between the initial stage and the sampling stage is controlled by a sequence of logic signals provided by the logic program as shown in Figure 5. The digital clock provides the program with so many equitemporal clock pulses per second (from 1 to 10^5) and the logic program changes this sequence of pulses into an alternating series of "High Signal" and "Low Signal" for every clock pulse. The "High Signal" and "Low Signal" are sensed through the hybrid interface by the digital computer which, in turn, controls the operation of the analog computer based on this alternating series. The integration will last for a period between two consecutive clock pulses.

After the nine probabilities at one space grid point and one particular time are obtained, integration proceeds for the next space grid point. New values of the intensities of sediment motion, ψ's, are sent from the digital computer memory to the analog computer through nine digital-analog converted channels (DAC) and the same procedure is repeated to obtain the nine probabilities for this new space grid point.

HYBRID COMPUTER SIMULATION

There are generally two phases in the development of models. The first phase involves incorporating into the entire model various model components which are based on mathematical equations and testing the effects of each component on the whole model and on the other components to see their behavior. In the second phase, the model is used in actual simulations. Measured input and control data will be used for calibration and testing of the processes modeled, and the model subsequently will be used for predictive purposes.

The model as a whole is being synthesized on a hybrid computer available at the Utah Water Research Laboratory. The model will be tested by simulating conditions within an ephemeral reach of the Walnut Gulch Watershed in southern Arizona. This is a highly instrumented watershed operated by the Southwest Watershed Research Center, Agricultural Research Service, Tucson, Arizona.

The ultimate aim of the model, however, is to be applicable not only to ephemeral streams in the Southwest, but to a wide variety of systems of erodible streams. Since field data are not yet available only the first phase has been carried out.

Simulation of a Stream Reach

The movement of flood wave and sediment is simulated in a reach which is 24,000 feet long. The average cross section is trapezoidal. Hypothetical input hydrograph and suspended sediment discharge at the upstream end of the reach are used to demonstrate the operation of the model. The bed load discharge at the upstream end can be computed directly by the model. To satisfy the stability criteria the time step Δt and space step Δx are taken as one minute and 1,200 feet, respectively. Figure 6 shows the inflows and simulated outflows of water, suspended sediment, and bed load, based on an average bed slope of 0.005, a mean grain diameter of 0.036 inches, a bed width of 50 feet, and a hydraulic conductivity (Darcy's K) of 0.0003 foot per second. The flood wave reaches the downstream end of the reach after 35 minutes. The discharges of water, suspended sediment, and bed load are considerably less than the inflows, because of the length of the reach and the high seepage rate through the stream bed. The effect of seepage on water discharge can be seen by comparing the areas enveloped by the inflow hydrograph and the time axis, and the outflow hydrograph and the time axis. Figure 7 shows the cumulative hydrographs and suspended sediment discharge graphs. About three fifths of the total amount of water input into the reach are lost into the ground. Figure 6 also shows that the peak of the suspended sediment graph occurs at about the same time as the peak of the mean velocity graph, while, as expected, the peak of the bed load graph lags behind

the peak of the hydrograph by about the same amount of time at the upstream end of the stream reach as at the downstream end. This means that the suspended sediment discharge tends to change instantaneously with the mean cross-sectional velocity, while the bed load, which is insensitive to the change in velocity, responds better to the changes in water discharge. These phenomena are illustrated by Figures 8, 9, 10, and 11, which show the profiles of the water discharge, the mean cross-sectional velocity, the bed load, and the suspended load, respectively. The explanation to the slow response of the bed load to the change in mean cross-sectional velocity is that the bed load is a function of the bed shear stress which responds better to the water discharge than to the mean cross-sectional velocity.

A sample of the probability profiles is shown in Figure 12 for the transfer of sediment from immobile bed state to bed load state. The profiles tend to have relatively flat lee-side slopes and the peaks stay at about the same level as time elapses. This also helps illustrate the slow response of bed load to changes in mean cross-sectional velocity.

When a flood moves down the stream channel, the velocity at the stream bed increases, although not as fast as the velocity in the main flow body. However, the resulting bed shear stress and normal stress due to velocity fluctuations may be high enough that sediment particles have tendency to move from lower states to upper states as can be seen in Figures 13, 14, and 15. In Figure 13, profiles of the probabilities of the transfer of sediment from the suspended load state Ⓐ to the same state or lower states show pronounced peaks and troughs. The probability of staying within the same state Ⓐ increases to the peak at about the same place as the peak of the corresponding water discharge profile, while the probabilities of going into the bed load state Ⓑ or the immobile bed state Ⓒ decrease to their minima at the same place. Figures 14 and 15 show that the probability of leaving the bed load state Ⓑ is zero and so is the probability of going from the immobile bed state Ⓒ to the suspended load state Ⓐ. The probability of going from state Ⓒ to state Ⓑ is very high, and the probability of staying within state Ⓑ is 100 percent. This suggests that the normal stress due to the upward velocity fluctuations at the stream bed is not high enough to lift the sediment particle into the suspended load state Ⓑ at the stream bed, and that the bed shear stress can easily cause the particle to slide and roll along the stream bed. This fact is as expected because only the median sediment size is being considered. In the next stage of investigation, an attempt will be made to extend the model to deal with all sediment size ranges. It should be noticed that, in Figure 15, the profile of the probability of leaving state Ⓒ for state Ⓑ maintains a plateau behind the front of the flood wave, which again shows the slow response of the bed load function to the mean cross-sectional velocity variation.

Sensitivity Analysis

Sensitivity analysis gives an insight into the model response to changing parameters by providing the investigator the knowledge on the degree of importance of each parameter. The procedure used in analyzing the sensitivity of the model consists in varying one parameter while keeping the others constant. This model consists mostly of functional relationships, such as friction factors, ratios between bed shear stress and normal turbulent stresses, and dynamic friction factor for the sediment particles. There are only two parameters that can be used for testing the model: the hydraulic conductivity of the stream bed, or Darcy's K, and the median sediment diameter. Although the average bed slope is not a parameter because it is a function of the stream bed elevation, it is useful to see the effects of changing slopes on the discharges of water, suspended sediment, and bed load, for a given hydraulic conductivity of the stream bed.

Figure 16 shows the effects of changing the hydraulic conductivity, Darcy's K, on the water discharge. For a K value of 0.0003 ft/sec, about two-thirds of the amount of water input into the reach, seeps through the stream bed. For a zero value of K, no water is lost through seepage. The outflow hydrographs preserve the same shape of peaks as the inflow hydrograph, although they are less in magnitude. This is due to the steep bed slope of .01. The effects of changing the median size of sediments can be seen in Figures 17 and 18. Increasing the median size of sediments tends to increase the time of rise of the hydrograph while the magnitude of the peak is preserved. The time of rise increases by about two minutes with a size increase of .001 foot. The graphs of the suspended sediment discharge at the downstream end show a reduction in the peak and an increase in the time of rise as the median size of sediments is increased. Finally, Figure 19 shows that an increase in the median size of sediments causes a decrease in bed load discharge and the peaks of the graphs come at about the same time.

The effects of bed slope on the water discharge is shown in Figure 20. A steeper bed slope corresponds to a higher discharge at the downstream end because of higher flow velocity and less depth, and therefore lower seepage rate. The rise is slower and the peak decreases with decreasing slope. The graphs of the suspended sediment discharge follow about the same pattern as the outflow hydrographs as can be seen in Figure 21. The bed slope affects the bed load discharge in about the same manner as the size of sediments do. Figure 22 indicates that the peaks of the bed load graphs occur at about the same time regardless of slope, however, their magnitude decreases considerably with decreasing slope.

CONCLUDING REMARKS

The major objective of the present phase of the study has been to develop a simulation model to integrate both the movements of flood and sediment flows down an unstable, erodible stream channel. An effort was made to apply stochastic processes to the description and evaluation of the transfer of sediments at the stream bed which cannot be adequately described in a deterministic way. The advantage of using Markov processes for this purpose is that the problem associated with separating the bed load zone from the suspended load zone can be overcome by considering states of sediment particles, which are suspended load state, bed load state, and immobile bed state. This stochastic part of the model provides the expected values of the transfer of sediments at the stream bed.

The development of the one-dimensional mathematical equations describing the movement of flood wave and suspended sediment was based on the principles of fluid mechanics by starting from the three-dimensional equations and arriving at the one-dimensional equations through space-integration.

Numerical methods were used to obtain the solution to these one-dimensional equations and a direct analog computer integration was adopted to obtain the solution to the Kolmogorov system, Equation (38), which provides the probabilities of the transfer of sediments at the stream bed. An analytical investigation of the stability of the difference schemes and the analog solution was conducted to obtain stability criteria for the solution.

Simulation of the dynamics of a reach of an erodible stream was done on an EAI* hybrid computing system and results have been presented and discussed.

From this phase of the study the following major conclusions can be drawn:

1. The integrated model describing the dynamics of erodible streams is feasible for field applications because the entire model reduces to being a function of the bed shear stress mainly.

2. Numerical solutions to the one-dimensional equations describing the water and suspended sediment flows are conditionally stable. The stability criteria do not increase the computation time enough as to cause the model to be unfeasible economically. The small time step Δt imposed by these criteria is, however, desirable when dealing with short time runoff processes

* Use of a trade name does not imply endorsement by Utah State University or the U.S. Department of Agriculture but is included for technical completeness.

and particularly the ephemeral stream in the Southwest where the hydrographs peak within a few minutes after inflow begins.

3. The analog computer is particularly suited to the simultaneous solution of the Kolmogorov system which consists of nine linear ordinary differential equations of the first order. The negative values of the intensity of the transfer of sediment within the same state cause the errors associated with the computation to decay exponentially with time.

4. The bed shear stress is the main factor which is controlling the stability of the numerical solutions. It limits the time step Δt to very small values which increase considerably the computation time. However, the fluctuations in the values of the bed shear stress term are critical only when the cross-sectional area of flow is small.

5. The suspended sediment discharge tends to change instantaneously with the water discharge, but there is a time lag in the bed load response.

6. The sentivity analysis on different parameters shows that the responses of the graphs of the water discharge, suspended sediment discharge, and bed load discharge agree with what might be expected from field observations.

7. This tentative model provides reasonable results. It can, therefore, be used in the second phase of the study, that is, using the model in actual simulations.

Although the model is considered as complete in a sense of entity, it is still in the tentative stages and further development and testing will be undertaken.

PARTIAL LIST OF SYMBOLS

SYMBOL	Definition
A	Cross-sectional area of flow
Ⓐ	Suspended load state at the stream bed
Ⓑ	Bed load state at the stream bed
Ⓒ	Immobile bed state at the stream bed
C	Overall average concentration of suspended sediment (volumetric)
$C/_{y=\eta_1} = C_B$	Bed load concentration
c	Point sediment concentration in three-dimensional field
C_D	Drag coefficient
D	Sediment diameter (equivalent from volume of sphere)
D_{mean}	Mean sediment diameter
D_{50}	Median sediment diameter
e	Mass diffusivity in the three-dimensional field
$\vec{F}$	Force vector on the particle
$F(x, y, z, t) = 0$	Boundary surface in the three-dimensional field
f	Friction factor
f'	Friction factor due to grain roughness
f''	Friction factor due to bed forms
G_{cx}	Longitudinal solid dispersivity
$\vec{g}$	Gravitational acceleration
h	Flow depth

PARTIAL LIST OF SYMBOLS (CONT.)

SYMBOL	Definition
h_c	Depth from free stream surface to centroid of flow cross-sectional area
I	Intensity of turbulence
$\vec{I}$	Identity vector
K	Hydraulic conductivity of the stream bed
L	Lateral flow into or from the channel per unit length
m	Mass of solid particle
N	Local total sediment transfer rate at the stream bed
P_{AB}	Probability that a particle moves from state Ⓐ to state Ⓑ
$\vec{P}$	Probability vector
p	Point pressure
Q	Total fluid discharge
$Q_{B\ vol}$	Volumetric bed load discharge
Q_{BS}	Volumetric rate of sediment exchange between the stream bed and the suspended load
$\vec{R}$	Vector flow across stream boundary surface
R_h	Hydraulic radius
S	Total seepage into or from the channel bed per unit length
T	Top width of flow
$T^{(e)}$	Reynolds stress tensor
U	Mean stream velocity

PARTIAL LIST OF SYMBOLS (CONT.)

Symbol	Definition
$\vec{V}_p$	Solid particle velocity vector at the interface
u', v', w'	Turbulent velocity fluctuations
α	Average angle of encounter between individual particles
β	Momentum correction factor for the velocity distribution in the main flow
β_L	Momentum correction factor for the lateral inflow
β_S	Momentum correction factor for the seepage
γ	Fluid specific weight
γ_s	Sediment specific weight
δ_{ij}	Kronecker delta symbol
η_1	Elevation of the stream bed above some datum
η_2	Elevation of the free surface of flow above some datum
κ	von Karman universal constant
μ	Fluid dynamic viscosity
λ	Ratio of the eddy mass diffusivity e to the eddy mass diffusivity e_m
ν	Kinematic fluid viscosity
ρ	Fluid density
ρ_s	Sediment density
σ_1	Coordinate of the right stream bank
σ_2	Coordinate of the left stream bank
τ_o	Bed shear stress

PARTIAL LIST OF SYMBOLS (CONT.)

SYMBOL	Definition
ϕ_x	Ratio of the root-mean-square of the longitudinal normal turbulent stress to the friction velocity at the stream bed
ϕ_y	Ratio of the root-mean-square of the vertical normal turbulent stress to the friction velocity at the stream bed
$\vec{\psi}$	Vector intensity of sediment motion at the stream bed

REFERENCES

1. Renard, K. G., and Hickock, R. B., "Sedimentation Research Needs in Semi-Arid Regions," Proc. of the ASCE, Vol. 93, No. HY1, pp. 45-60, January, 1967.

2. Sakhan, K. S., "Simulation of the Dynamics of Erodible Streams," Ph.D. Dissertation, Utah State University, Logan, Utah, 1971.

3. Chen, C. L., "Sediment Dispersion in Flow with Moving Boundaries," Proc. of the ASCE, Vol. 96, No. HY8, Paper 8287, 1971.

4. Bagnold, R. A., "Flow of Cohesionless Grains in Fluids," Royal Society [London] Philos. Trans., Vol. 249, pp. 235-297, 1956.

5. Laufer, J., "The Structuve of Turbulence in Fully Developed Pipe Flow," National Advisory Committee for Aeronautics, Technical Report 1174, p. 17, 1954.

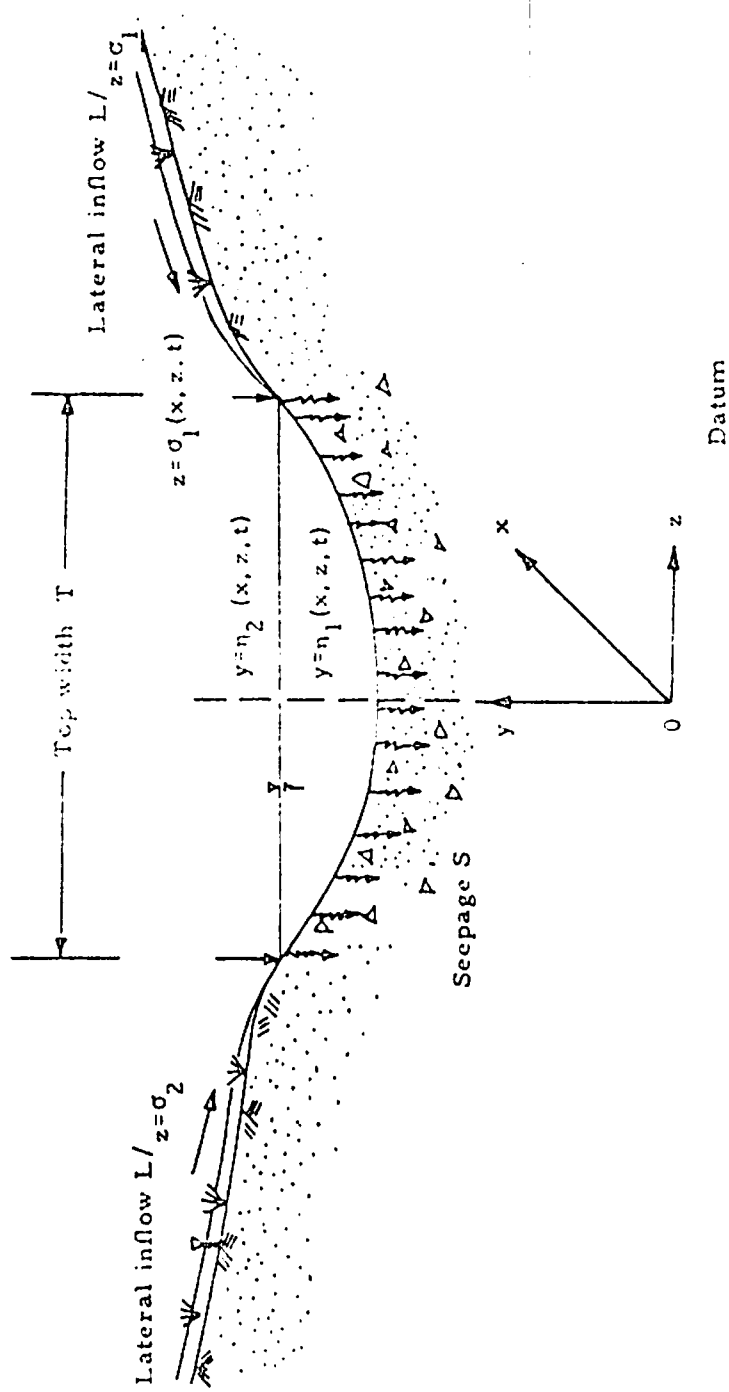

Fig. 1.a. Illustration of the Stream Coordinates

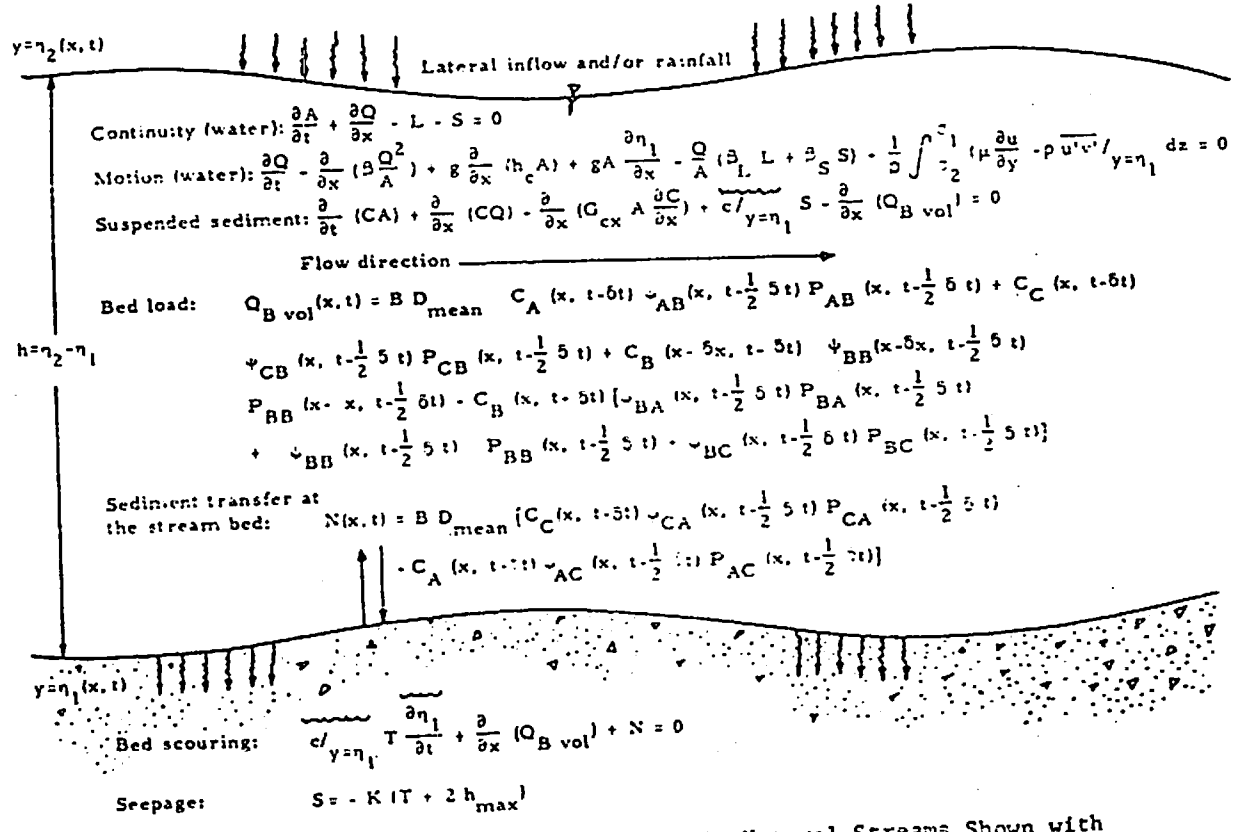

Continuity (water): $\frac{\partial A}{\partial t} + \frac{\partial Q}{\partial x} - L - S = 0$

Motion (water): $\frac{\partial Q}{\partial t} - \frac{\partial}{\partial x}\left(\beta \frac{Q^2}{A}\right) + g\frac{\partial}{\partial x}(h_c A) + gA\frac{\partial \eta_1}{\partial x} - \frac{Q}{A}(\beta_L L + \beta_S S) - \frac{1}{\rho}\int_{\eta_2}^{\eta_1}\left(\mu\frac{\partial u}{\partial y} - \rho\,\overline{u'v'}\right)_{y=\eta_1} dz = 0$

Suspended sediment: $\frac{\partial}{\partial t}(CA) + \frac{\partial}{\partial x}(CQ) - \frac{\partial}{\partial x}\left(G_{cx} A \frac{\partial C}{\partial x}\right) + c/_{y=\eta_1}\, S - \frac{\partial}{\partial x}(Q_{B\,vol}) = 0$

Bed load: $Q_{B\,vol}(x,t) = B\,D_{mean}\; C_A(x, t-\delta t)\,\psi_{AB}(x, t-\frac{1}{2}\delta t)\,P_{AB}(x, t-\frac{1}{2}\delta t) + C_C(x, t-\delta t)$

$\psi_{CB}(x, t-\frac{1}{2}\delta t)\,P_{CB}(x, t-\frac{1}{2}\delta t) + C_B(x-\delta x, t-\delta t)\;\psi_{BB}(x-\delta x, t-\frac{1}{2}\delta t)$

$P_{BB}(x-x, t-\frac{1}{2}\delta t) - C_B(x, t-\delta t)\,[\psi_{BA}(x, t-\frac{1}{2}\delta t)\,P_{BA}(x, t-\frac{1}{2}\delta t)$

$+\;\psi_{BB}(x, t-\frac{1}{2}\delta t)\;P_{BB}(x, t-\frac{1}{2}\delta t) + \psi_{BC}(x, t-\frac{1}{2}\delta t)\,P_{BC}(x, t-\frac{1}{2}\delta t)]$

Sediment transfer at the stream bed: $N(x,t) = B\,D_{mean}\,[C_C(x, t-\delta t)\,\psi_{CA}(x, t-\frac{1}{2}\delta t)\,P_{CA}(x, t-\frac{1}{2}\delta t)$

$- C_A(x, t-\delta t)\,\psi_{AC}(x, t-\frac{1}{2}\delta t)\,P_{AC}(x, t-\frac{1}{2}\delta t)]$

Bed scouring: $c/_{y=\eta_1}\, T\frac{\partial \eta_1}{\partial t} + \frac{\partial}{\partial x}(Q_{B\,vol}) + N = 0$

Seepage: $S = -K\,(T + 2\,h_{max})$

Fig. 1.b. Integrated Sediment Movement in Natural Streams Shown with Equations which Describe Each Component Process

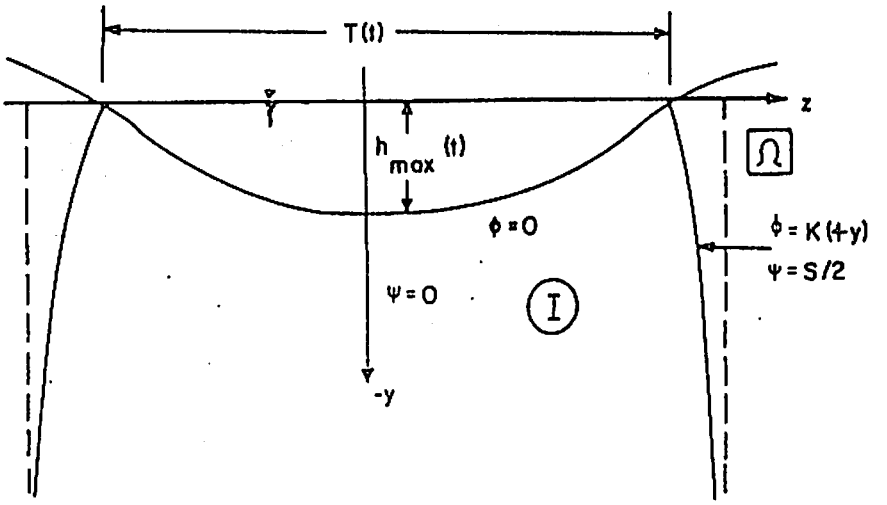

Fig. 2. Seepage from open channels with water table at infinite depth

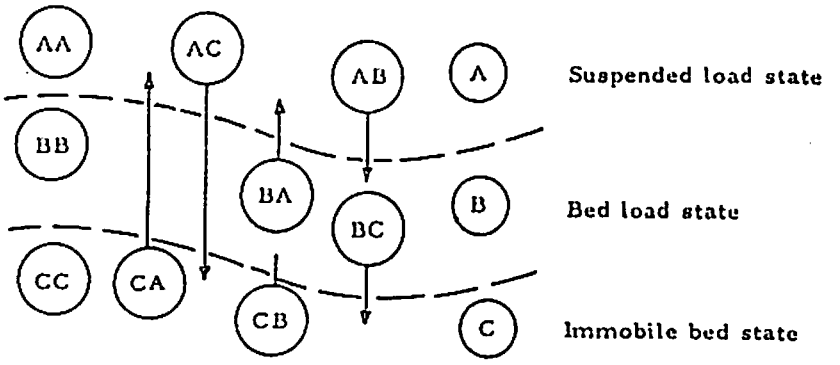

Fig. 3. Illustration of Sediment Transfer at the Stream Bed

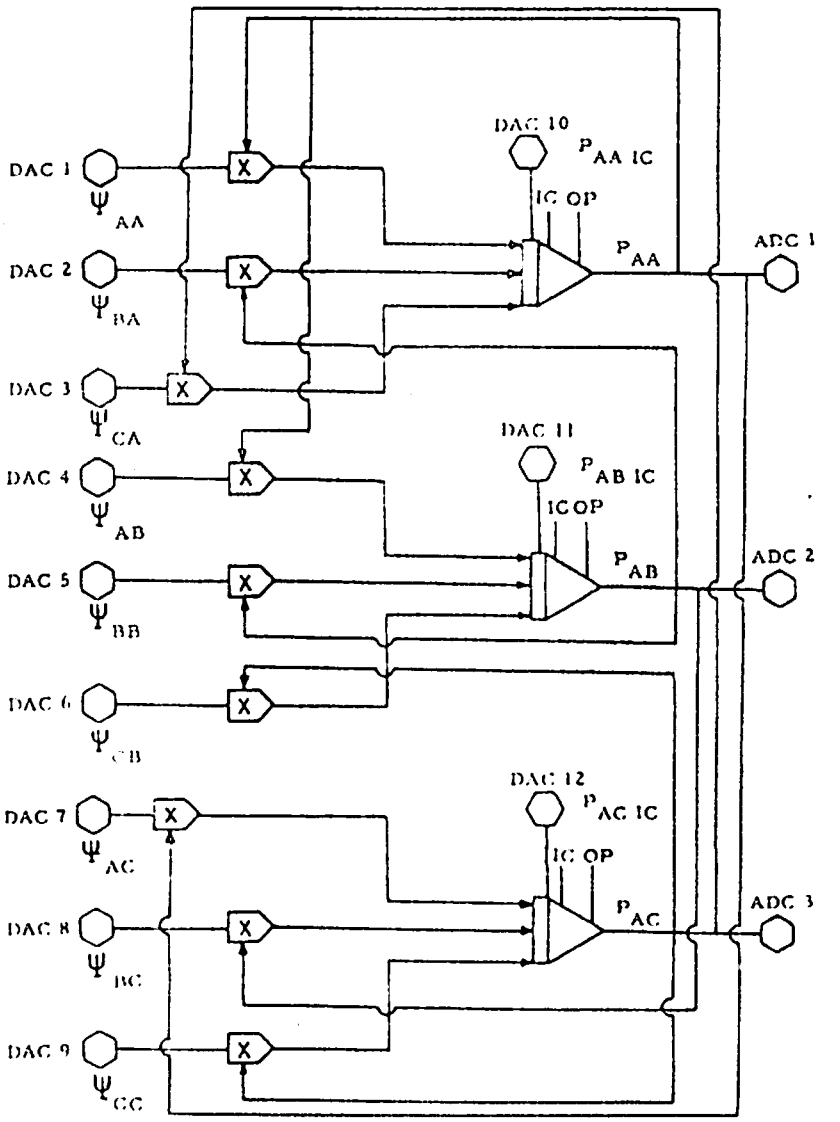

Fig. 4. Sample Analog Diagram for the Kolmogorov System

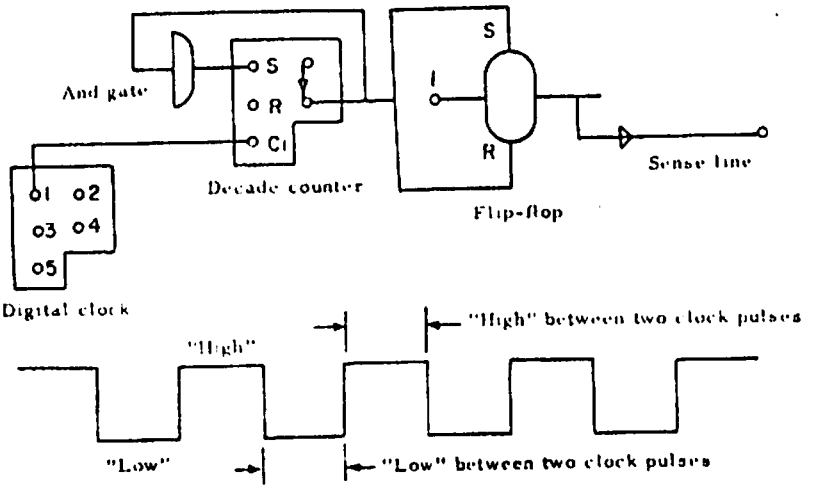

Fig. 5. Logic Program

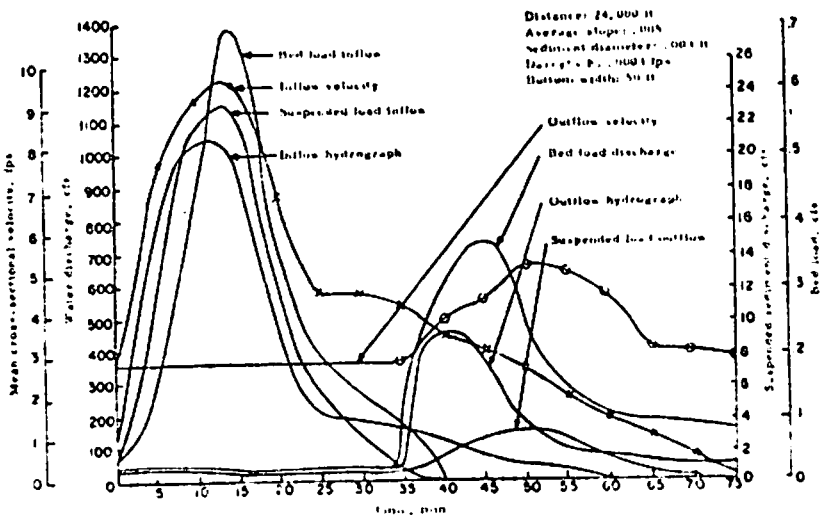

Fig. 6. Inflow and Simulated Outflows

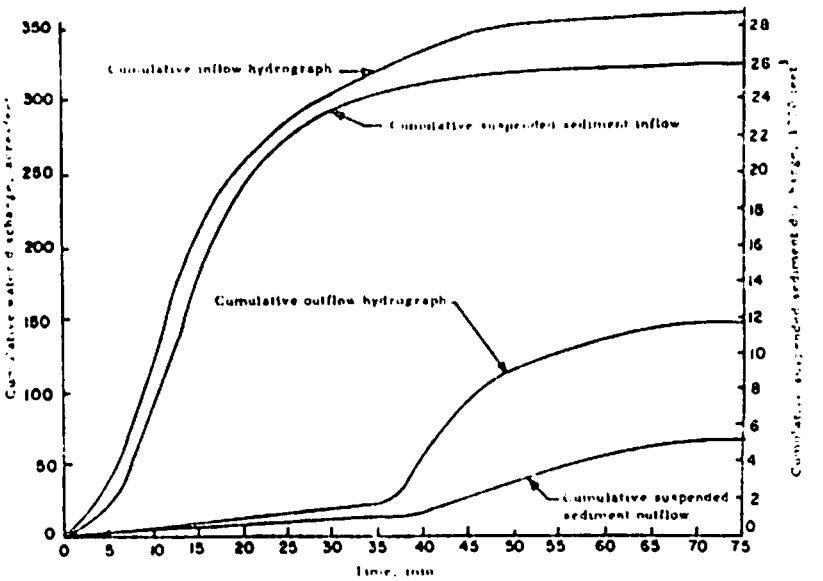

Fig. 7. Cumulative Hydrograph and Suspended Sediment Graph

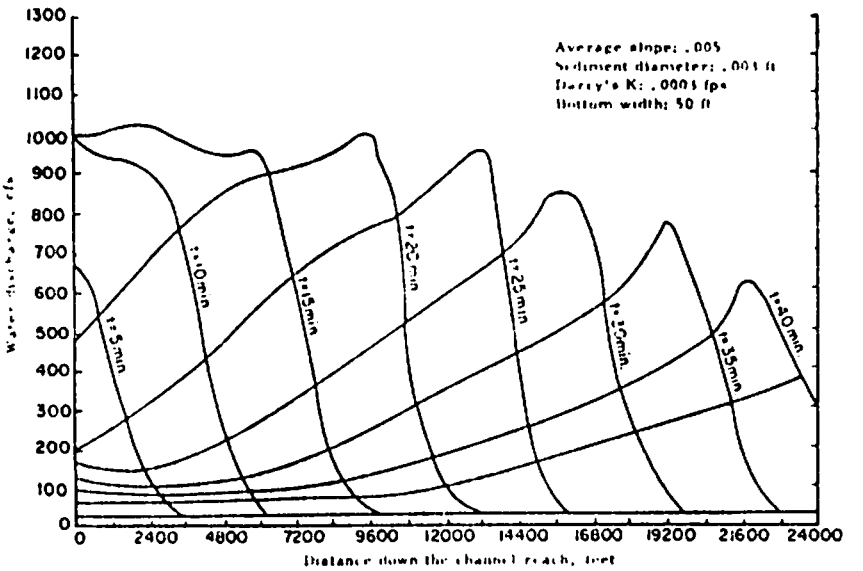

Fig. 8. Water Discharge Profiles

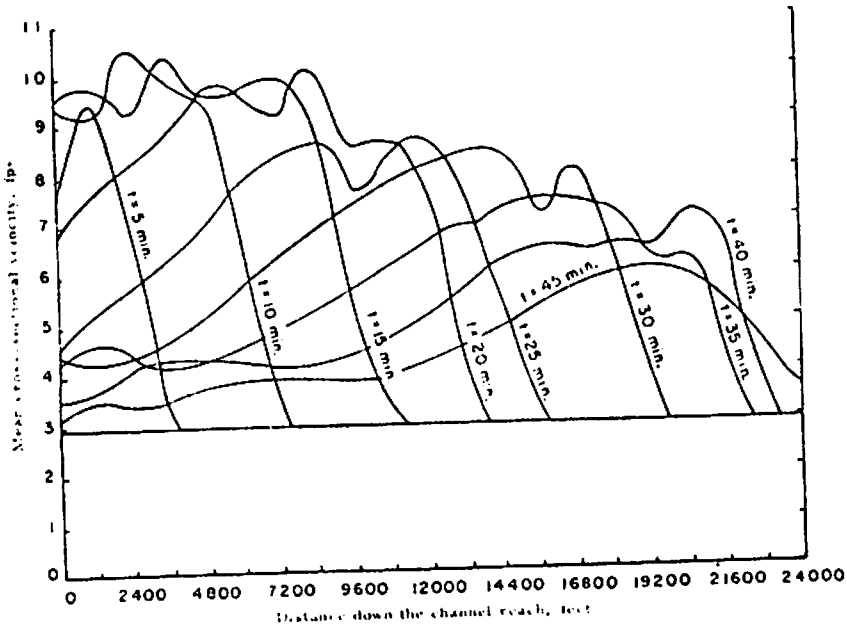

Fig. 9. Mean Cross-Sectional Velocity Profiles

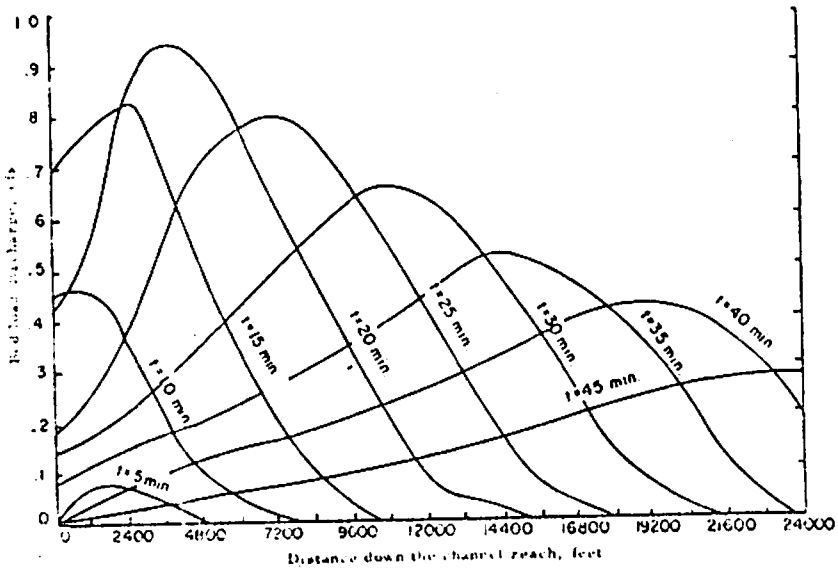

Fig. 10. Bed Load Discharge Profiles

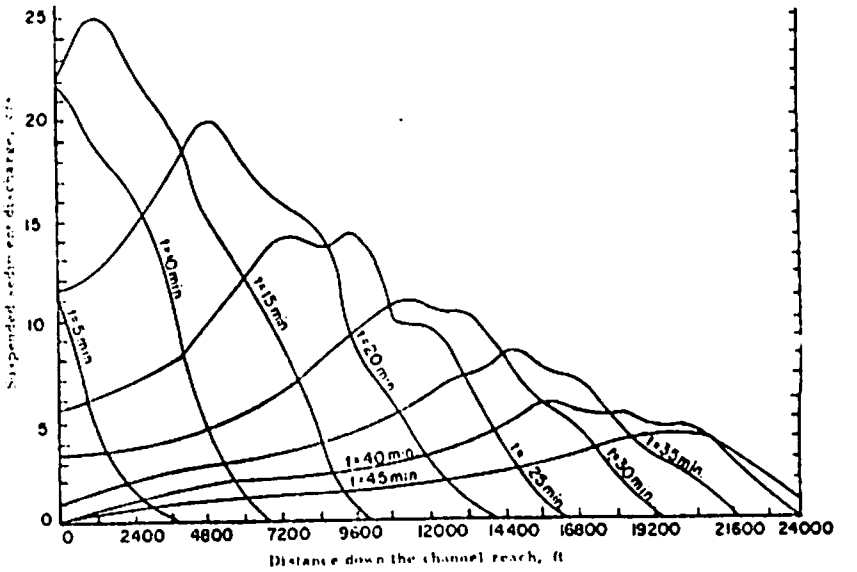

Fig. 11. Suspended Load Profiles

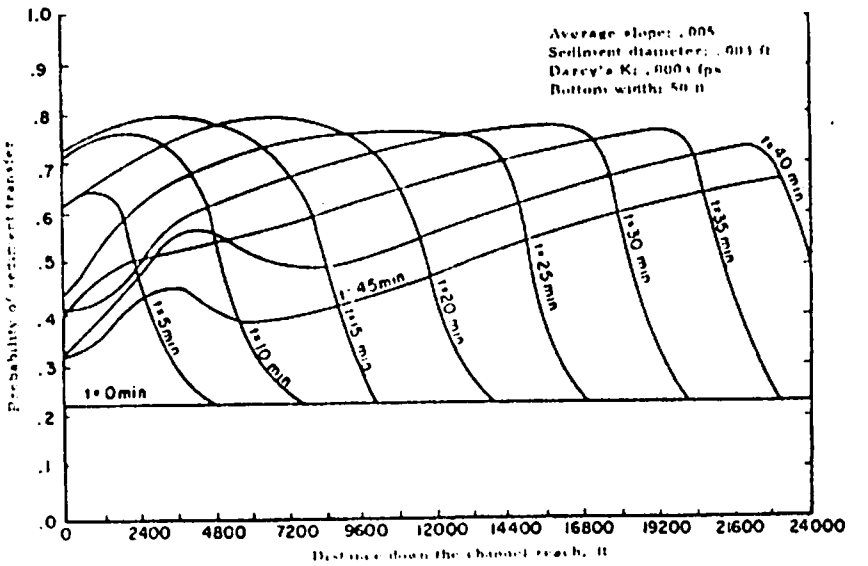

Fig. 12. Profiles of the Probability of the Transfer of Sediment from the Immobile Bed State to Bed Load State, P_{CB}

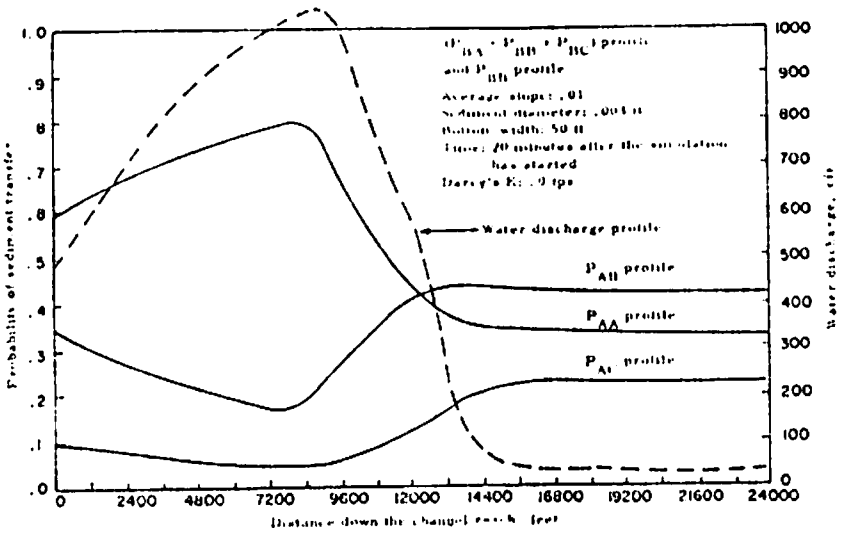

Fig. 13. Profiles of the Probabilities of the Transfer of Sediment from the Suspended Load State to the Suspended Load State, P_{AA}, to the Bed Load State, P_{AB}, and to the Immobile Bed State, P_{AC}, in Relation to Water Discharge Profile

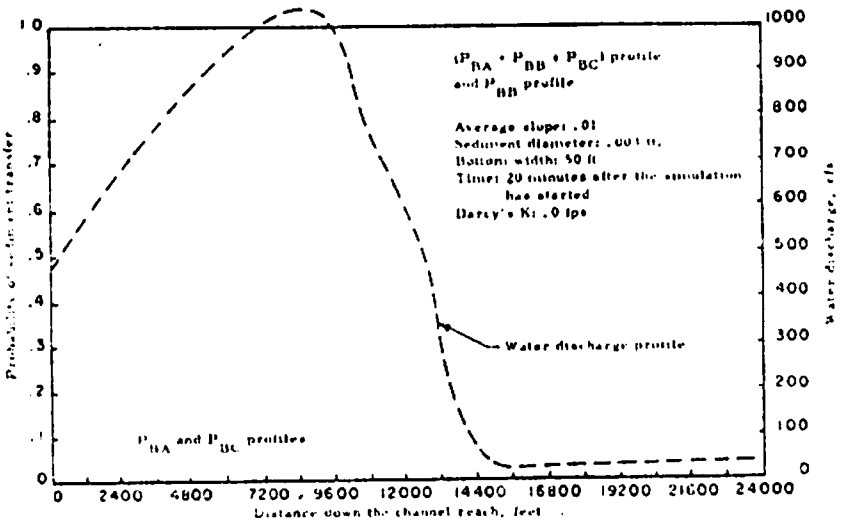

Fig. 14. Profiles of the Probabilities of the Transfer of Sediment from the Bed Load State to the Su pended Load State, P_{BA}, to the Bed Load State, P_{BB}, and to the Immobile Bed State, P_{BC}, in Relation to Water Discharge Profile

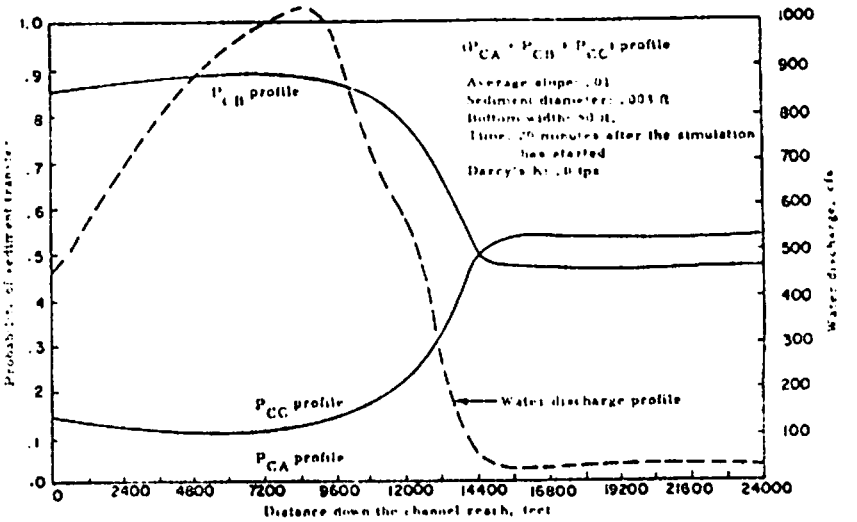

Fig. 15. Profiles of the Probabilities of the Transfer of Sediment from the Immobile Bed State to the Suspended Load State, P_{CA}, to the Bed Load State, P_{CB}, and to the Immobile Bed State, P_{CC}, in Relation to the Water Discharge Profile

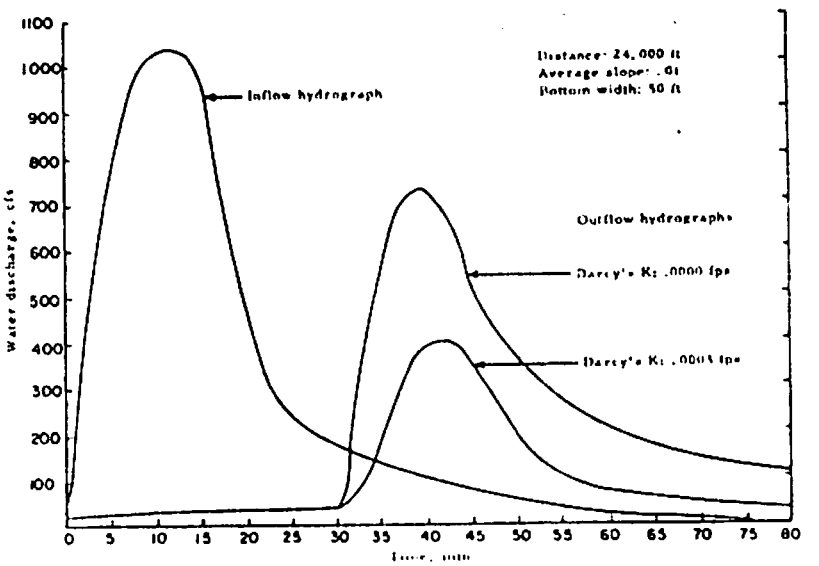

Fig. 16. Effects of Seepage on the Water Discharge

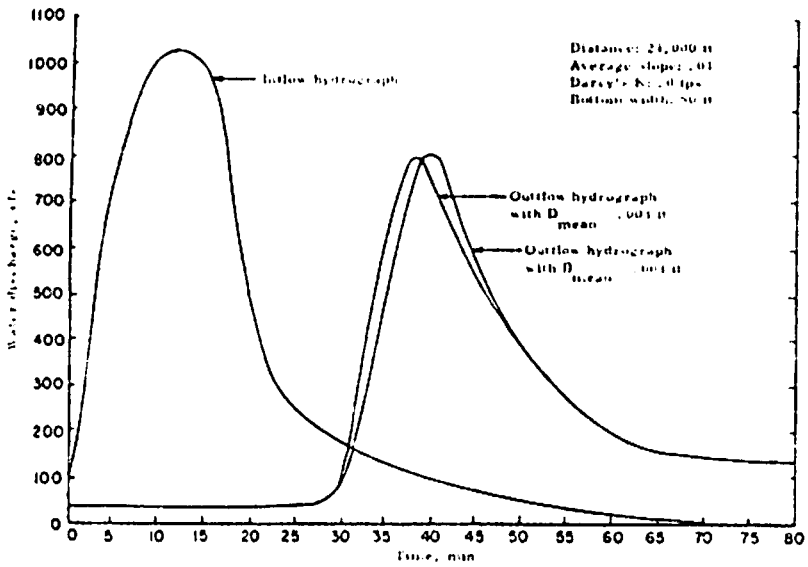

Fig. 17. Effects of Bed Grain Size on the Water Discharge

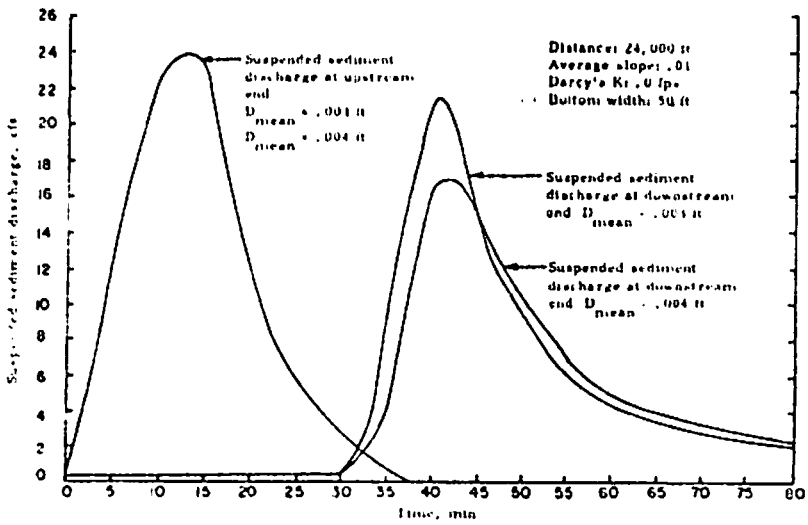

Fig. 18. Effects of Bed Material Size on the Suspended Sediment Discharge

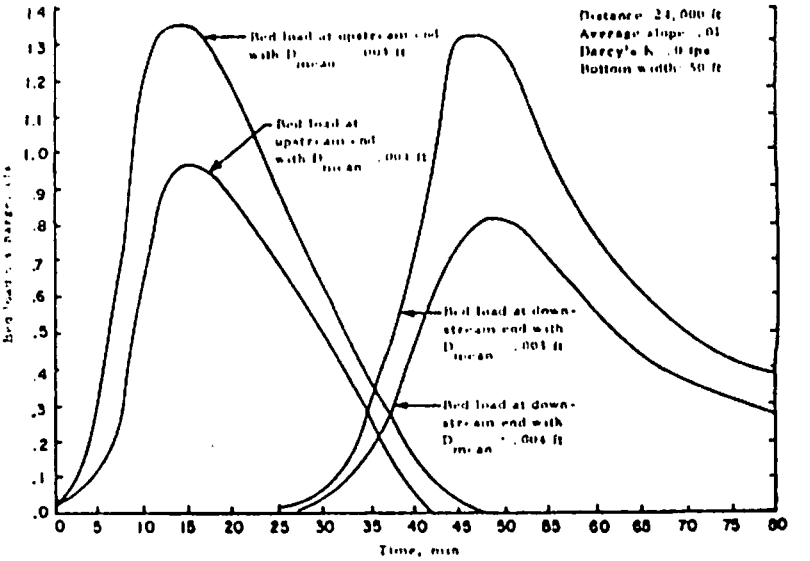

Fig. 19. Effects of the Bed Grain Size on the Bed Load Discharge

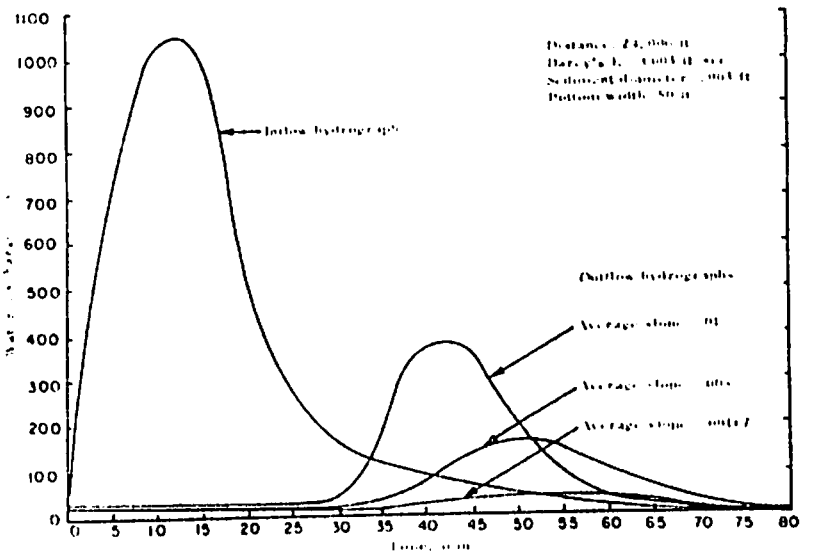

Fig. 20. Effects of the Average Bottom Slope on the Water Discharge

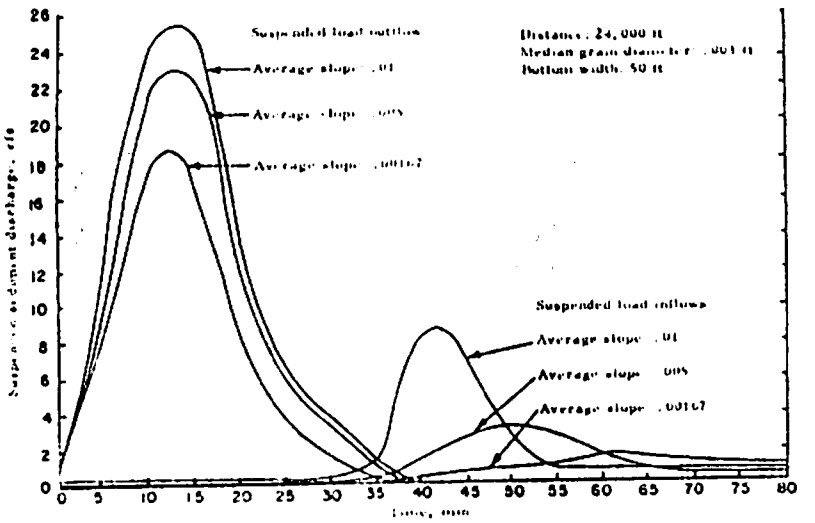

Fig. 21. Effects of Changing Slopes on the Suspended Sediment Discharge

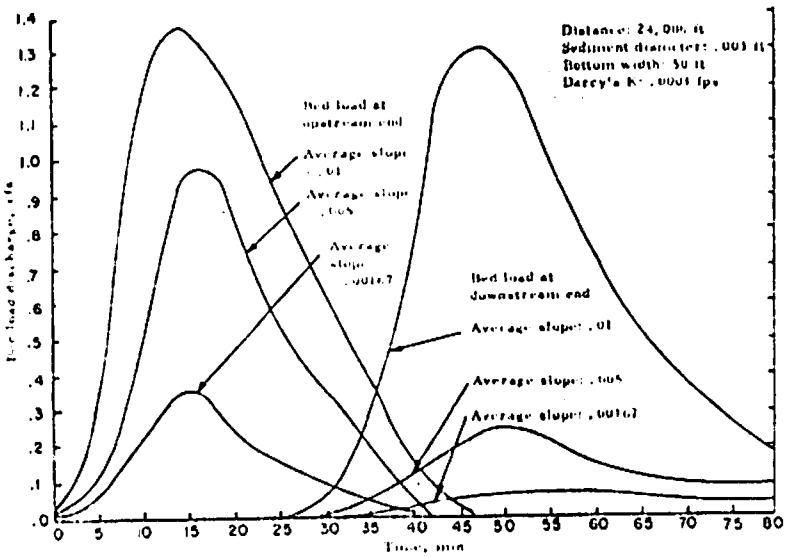

Fig. 22. Effects of Changing Slopes on the Bed Load Discharge